

1 **Investigation of water adsorption and hygroscopicity of atmospherically**
2 **relevant particles using a commercial vapor sorption analyzer**

3

4 Wenjun Gu^{1,4}, Yongjie Li², Jianxi Zhu³, Xiaohong Jia^{1,4}, Qin hao Lin¹, Guohua Zhang¹, Xiang
5 Ding¹, Wei Song¹, Xinhui Bi¹, Xinming Wang^{1,5}, Mingjin Tang^{1,*}

6

7 1 State Key Laboratory of Organic Geochemistry and Guangdong Key Laboratory of
8 Environmental Protection and Resources Utilization, Guangzhou Institute of Geochemistry,
9 Chinese Academy of Sciences, Guangzhou 510640, China

10 2 Department of Civil and Environmental Engineering, Faculty of Science and Technology,
11 University of Macau, Avenida da Universidade, Taipa, Macau, China

12 3 CAS Key Laboratory of Mineralogy and Metallogeny and Guangdong Provincial Key
13 Laboratory of Mineral Physics and Material Research & Development, Guangzhou Institute of
14 Geochemistry, Chinese Academy of Sciences, Guangzhou 510640, China

15 4 University of Chinese Academy of Sciences, Beijing 100049, China

16 5 Center for Excellence in Regional Atmospheric Environment, Institute of Urban
17 Environment, Chinese Academy of Sciences, Xiamen 361021, China

18

19 Correspondence: M. J. Tang (Email: mingjintang@gig.ac.cn)

20

21 **Abstract**

22 Water adsorption and hygroscopicity are among the most important physicochemical
23 properties of aerosol particles, largely determining their impacts on atmospheric chemistry,
24 radiative forcing, and climate. Measurements of water adsorption and hygroscopicity of
25 nonspherical particles under subsaturated conditions are non-trivial because many widely used
26 techniques require the assumption of particle sphericity. In this work we describe a method to
27 directly quantify water adsorption and mass hygroscopic growth of atmospheric particles for
28 temperature in the range of 5-30 °C, using a commercial vapor sorption analyzer. A detailed
29 description of instrumental configuration and experimental procedures, including relative
30 humidity (RH) calibration, is provided first. It is then demonstrated that for $(\text{NH}_4)_2\text{SO}_4$ and
31 NaCl, deliquescence relative humidities (DRHs) and mass hygroscopic growth factors
32 measured using this method show good agreements with experimental and/or theoretical data
33 from literature. To illustrate its ability to measure water uptake by particles with low
34 hygroscopicity, we used this instrument to investigate water adsorption by $\text{CaSO}_4 \cdot 2\text{H}_2\text{O}$ as a
35 function of RH at 25 °C. The mass hygroscopic growth factor of $\text{CaSO}_4 \cdot 2\text{H}_2\text{O}$ at 95% RH,
36 relative to that under dry conditions ($\text{RH} < 1\%$), was determined to be $(0.450 \pm 0.004)\%$ (1σ).
37 In addition, it is shown that this instrument can reliably measure a relative mass change of
38 0.025%. Overall, we have demonstrated that this commercial instrument provides a simple,
39 sensitive and robust method to investigate water adsorption and hygroscopicity of atmospheric
40 particles.

41

42 **1 Introduction**

43 Atmospheric aerosol particles, directly emitted by natural and anthropogenic processes or
44 secondarily formed in the atmosphere, have significant impacts on air quality, visibility, human
45 health, and radiative and energy balance of the Earth system (Pöschl, 2005; Seinfeld and Pandis,
46 2006). The ability to uptake water is among the most important physicochemical properties of
47 aerosol particles, and it largely determines their impacts on atmospheric chemistry and climate
48 (Martin, 2000; Rubasinghege and Grassian, 2013; Farmer et al., 2015; Tang et al., 2016). The
49 ability of aerosol particles to uptake water depends on particle composition, relative humidity
50 (RH), and temperature (Martin, 2000; Tang et al., 2016). Under subsaturated conditions (RH
51 <100%), the ability to uptake water is typically called water adsorption in surface science and
52 hygroscopicity in aerosol science (Tang et al., 2016). Under supersaturated conditions, aerosol
53 particles can be activated to cloud droplets (McFiggans et al., 2006; Petters and Kreidenweis,
54 2007) and ice particles if temperature is below 0 °C (Pruppacher and Klett, 1994; Vali et al.,
55 2015).

56 Hygroscopicity of atmospheric particles has been extensively investigated by a large
57 number of studies, and many experimental techniques have been developed. These techniques
58 have been summarized and discussed by a very recent review paper (Tang et al., 2016), and
59 here we only mention widely used ones. For airborne monodisperse particles typically
60 produced by a differential mobility analyzer (DMA), the hygroscopicity can be determined by
61 measuring their diameters at dry (typically at RH <15% or lower) and humidified conditions
62 (Swietlicki et al., 2008; Freedman et al., 2009; Robinson et al., 2013; Lei et al., 2014). Typically,
63 the diameter change is determined by using a scanning particle mobility sizer (in which
64 mobility diameters are measured) (Vlasenko et al., 2005; Swietlicki et al., 2008; Herich et al.,
65 2009; Koehler et al., 2009; Wu et al., 2011) or aerosol extinction-cavity ring down
66 spectrometry (in which optical diameters are measured) (Freedman et al., 2009; Attwood and

67 Greenslade, 2011). These techniques require an underlying assumption that particles are
68 spherical. However, a few important types of particles in the troposphere, including mineral
69 dust and soot, are known to be non-spherical (Veghte and Freedman, 2012; Ardon-Dryer et al.,
70 2015). Therefore, although these techniques can provide useful information, it is difficult to
71 quantitatively determine the amounts of water associated with non-spherical particles at a given
72 RH (Tang et al., 2016). Single particle levitation techniques, which measure light scattering
73 intensity to determine the size (and thus the hygroscopic growth) of levitated particles, also
74 have similar drawbacks (Krieger et al., 2012).

75 There are several techniques which can be applied to quantify the amount of water
76 associated with non-spherical particles at given temperature and RH. For example, adsorbed
77 water can be measured by FTIR by its IR absorption at around 3400 and 1645 cm^{-1} (Goodman
78 et al., 2001; Frinak et al., 2005; Ma et al., 2010a). However, it is non-trivial to convert IR
79 absorption intensity to the amount of adsorbed water (Schuttlefield et al., 2007a; Tang et al.,
80 2016). Several previous studies have used quartz crystal microbalance (QCM) to measure DRH
81 and mass hygroscopic growth of particles (Schuttlefield et al., 2007b; Arenas et al., 2012; Liu
82 et al., 2016; Yeşilbaş and Boily, 2016). The frequency change of the quartz crystal in a QCM,
83 according to the Sauerbrey equation, is proportional to the change in mass of particles loaded
84 on the crystal (Schuttlefield et al., 2007b). In addition, the amount of water associated with
85 particles at a given RH can also be determined by measuring the change in water vapor pressure
86 before and after exposure of particles to water vapor (Ma et al., 2010b; Ma et al., 2012), in a
87 manner similar to determination of Brunauer-Emmett-Teller surface area. In theory the
88 electrodynamic balance can be used to investigate the mass hygroscopic growth of non-
89 spherical particles (Chan et al., 2008; Lee et al., 2008; Pope, 2010; Griffiths et al., 2012). To
90 our knowledge, however, this technique has not been applied to mineral dust and soot particles
91 yet.

92 In this work we have developed an experimental method to investigate water adsorption
93 and hygroscopicity of atmospheric particles, using a vapor sorption analyzer which is
94 commercially available. We note that two groups have used similar techniques to measure
95 water adsorption by CaCO₃ and Arizona Test dust (Gustafsson et al., 2005) and DRH of
96 malonic acid, sodium oxalate and sodium malonate (Beyer et al., 2014; Schroeder and Beyer,
97 2016). Nevertheless, the performance of this technique has never been systematically evaluated.
98 To validate this experimental method, we have determined DRHs of six compounds as a
99 function of temperature from 5 to 30 °C, and the measured DRHs, varying from ~20% to ~90%
100 RH, show excellent agreement with literature values. In addition, mass hygroscopic growth
101 factors (MGF) of (NH₄)₂SO₄ and NaCl have been measured as a function of RH at 25 and 5 °C,
102 and the measured MGF agree very well with those predicted by the E-AIM model
103 (<http://www.aim.env.uea.ac.uk/aim/aim.php>; last accessed: 11 January 2017). Detailed
104 description of the E-AIM model can be found elsewhere (Clegg et al., 1998; Friese and Ebel,
105 2010). Hygroscopic growth factors, calculated using the E-AIM model, has been widely used
106 to compare with experimental measurements to verify the performance of a variety of
107 instruments, techniques and/or methods developed for hygroscopic growth studies (Pope et al.,
108 2010; Lei et al., 2014; Estillore et al., 2016). We show that this instrument can measure a
109 relative mass change (due to water uptake) of <0.025% within 6 hours and <0.05% within 24
110 hours, and the accuracy of mass change measurement is mainly limited by baseline drifts.
111 These features make this instrument particularly useful for laboratory studies of water
112 adsorption by nonspherical particles and/or particles with low hygroscopicity.

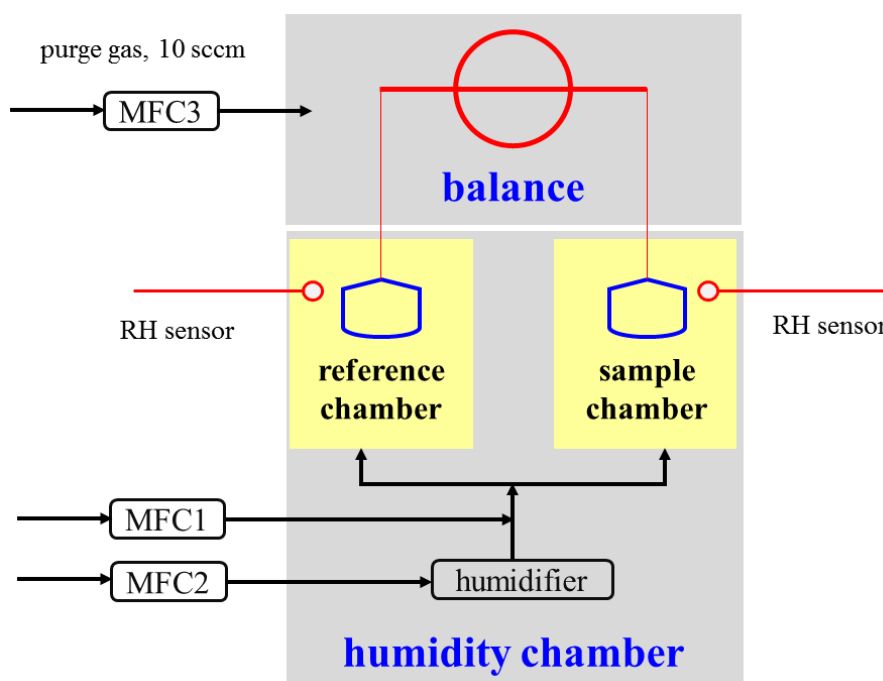
113 **2 Experimental section**

114 The instrument used in this work is a vapour sorption analyser (Q5000SA) manufactured
115 by TA Instruments (New Castle, DE, USA). The first part of this section provides a general

116 description of this instrument, and the second part describes experimental methods used in this
117 work.

118 2.1 Instrument description

119 Figure 1 shows the schematic diagram of the vapor sorption analyzer used in this work to
120 measure hygroscopicity and water adsorption of particles of atmospheric relevance. This
121 instrument consists of two main parts: 1) a high-precision balance used to measure the mass of
122 samples; 2) a humidity chamber in which temperature and RH can be precisely regulated and
123 also monitored online.



124
125 **Figure 1.** Schematic diagram of Q5000SA used in this work. MFC: mass flow controller. High
126 purity N₂ is used for all the three gas flows regulated by MFC1, MFC2, and MFC3, respectively.

127 2.1.1 High-precision balance

128 The balance simultaneously measures the mass of an empty pan (serving as a reference)
129 and a sample pan which contains particles under investigation. Each pan is connected to the
130 balance by a hang-down wire which has a hook at the lower end to hold the pan. The balance
131 is housed in a chamber which is temperature regulated. To avoid moisture condensation, the

132 balance chamber is purged with a 10 sccm (standard cubic centimetre per min) N₂ flow
133 regulated by a mass flow controller (MFC3).

134 The balance has a dynamic range of 0-100 mg. Typical dry mass of particles used in our
135 experiments are in the range of 1-10 mg so that the total mass of particles, due to adsorption of
136 water at high RH, does not exceed the upper limit of mass range. Powdered particles are
137 transferred into the sample pan using a small stainless-steel spatula. The mass of the sample
138 would not affect the measured mass ratio of dry particles to associated water under a given
139 condition; however, it would take more time to reach the equilibrium if the sample mass is
140 larger. The stated sensitivity of the balance is <0.1 µg with a weighing accuracy of ±0.1%, a
141 weighing precision of ±0.01%, and a signal resolution of <0.01 µg. The 24-h baseline drift is
142 stated to be <5 µg for an empty metalized quartz pan at 25 °C and 20% RH. This is equivalent
143 to a relative mass change of <0.05% if the sample mass is 10 mg. As shown Section 3.3,
144 experimental tests do suggest that such performance can be reached.

145 **2.1.2 Humidity chamber**

146 The humidity chamber is used to regulate the temperature and RH under which
147 hygroscopicity and/or water adsorption of particles are investigated. Inside the humidity
148 chamber are housed a reference chamber (in which an empty pan is connected to the balance)
149 and a sample chamber (in which a sample pan is connected to the balance). A dry N₂ flow
150 (regulated by MFC2) is delivered through a humidifier and then mixed the second dry N₂ flow
151 (regulated by MFC1). The total flow is set to 200 sccm, and the ratio of these two flows can be
152 adjusted in order to regulate the final RH. After mixing, the flow is then split into two flows,
153 one delivered into the reference chamber and the other into the sample chamber. Therefore,
154 both chambers should have the same temperature and RH. Temperature inside the humidity
155 chamber can be adjusted from 5 to 85 °C with a stated stability of ±0.1 °C, and RH can be
156 varied between 0 and 98%. High accuracy in RH control, with a stated absolute accuracy of

157 $\pm 1\%$, is achieved by precisely controlling the dry and humidified N₂ flow rates, using mass
158 flow controllers regularly calibrated. The accuracy of RH control is routinely checked by
159 measurement of the DRH of NaBr, as detailed in Section 3.1 In addition, as shown in Figure 1,
160 two capacitance RH sensors are used to check relative humidity in the chamber.

161 The main advantage of using a reference chamber and a sample chamber is that the amount
162 of water adsorbed by the empty pan and the attached wire can be simultaneously determined
163 (and automatically subtracted using the provided software) under the same condition when
164 water uptake by particles under investigation is being measured. In addition, the effect of
165 buoyancy, which varies with RH (Beyer et al., 2014; Schroeder and Beyer, 2016), is also
166 automatically taken into account by using an empty pan as the reference. Semispherical quartz
167 crucibles with a volume of 180 μL , provided by the manufacturer, are used in this work as
168 sample pans.

169 **2.1.3 Other features**

170 Q5000SA is equipped with a programmable autosampler designed to deliver sample pans
171 into the humidity chamber. The autosampler can host up to 10 sample pans; however, in order
172 to minimize contamination by lab air, only one sample pan is uploaded into the autosampler
173 immediately prior to the measurement. The instrument status is displayed on a touch screen for
174 local operation. Q5000SA can also communicate with a computer via Ethernet. Two software
175 packages are provided by the manufacturer: 1) TA Instrument Explorer Q Series is used to
176 control the instrument, program measurement procedures, and log experimental data; 2) TA
177 Universal Analysis can be used for graphing experimental data in real time, data analysis, and
178 exporting data. Experimental data can be sampled with frequencies up to 1 Hz.

179 **2.2 Experimental procedures**

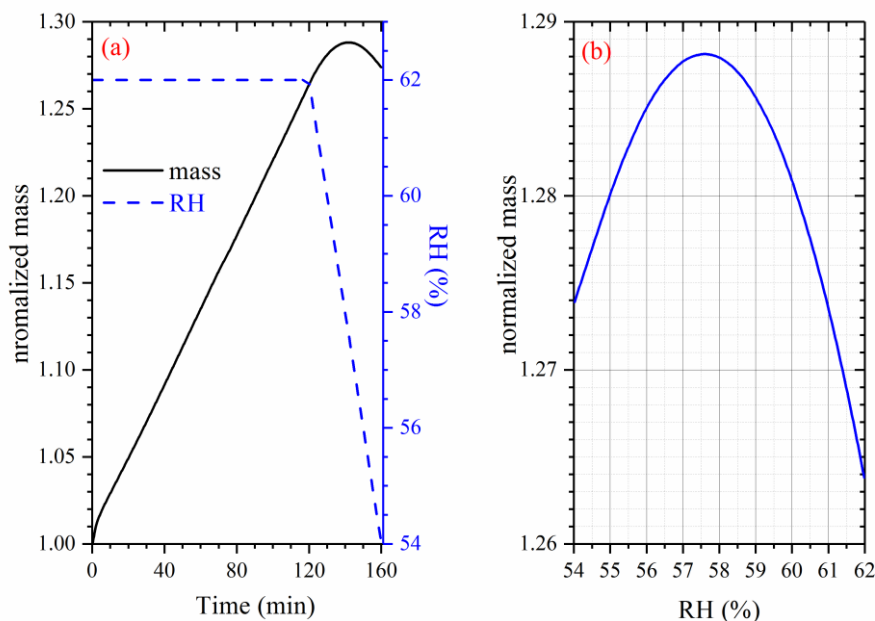
180 In our work two major experimental protocols are developed to 1) determine the DRH and
181 2) quantify water adsorption and/or mass hygroscopic growth. Corresponding experimental
182 procedures are detailed below.

183 **2.2.1 DRH determination**

184 Based on the standard recommended by American Society for Testing and Materials
185 International (ASTM, 2007) and TA Instruments (Waguespack and Hesse, 2007), an
186 experimental method has been developed in this work to determine the DRH of a given sample,
187 and it consists of the following steps. After the sample pan is properly located in the humidity
188 chamber, temperature is set to the given value. After temperature is stabilized, RH is set to a
189 value which is ~5% (when change/difference in RH is mentioned in this work, it always means
190 the absolute value) higher than the anticipated DRH and the system is equilibrated for 120 min.
191 **For example, the DRH of NaBr is expected to be around (57-58)%, and RH was set to 62%**
192 **from 0 to 120 min, as shown in Figure 2a. In the last step, RH is linearly decreased with a rate**
193 **of 0.2% per min to a value which is ~5% lower than the anticipated DRH. For example, as**
194 **shown in Figure 2a, RH was decreased from 62% at 120 min to 54% at 160 min, and the RH**
195 **decrease rate was 0.2% per min.**

196 Figure 2a shows changes of RH and sample mass (normalized to that at 0 min) as a function
197 of time in an experiment to measure the DRH of NaBr at 25 °C. RH was kept at 62% in the
198 first 120 min during which the sample mass increased with time. After that, RH was linearly
199 decreased to 54% with a rate of 0.2% RH per min, and during this period the sample mass first
200 continued to increase to a maximum value and then decreased with time. The sample mass in
201 the second period (120-160 min, as shown in Figure 2a) is plotted as a function of RH, and the
202 RH (57.6% in this case) at which the sample mass reached the maximum value is equal to the
203 measured DRH (ASTM, 2007). Measurement of a DRH usually takes ~3 h in total, and

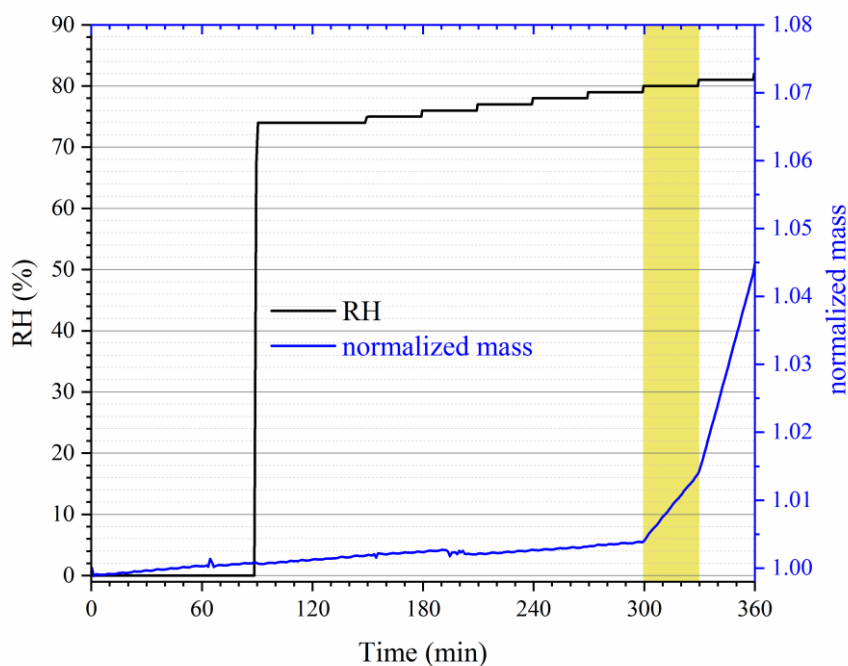
204 experimental data such as RH and sample mass are recorded with a time resolution of 10 s. If
 205 the DRH is unknown, we can increase the upper RH and decrease the lower RH used in the
 206 measurement so that the DRH falls into the RH range. Increasing RH range used in the
 207 measurement will of course lead to the increase of experimental time required.



208
 209 **Figure 2.** Typical experimental data in determination of DRH at a given temperature (NaBr at
 210 25 °C as an example) using Q5000SA by linearly decreasing RH. (a): Change of normalized
 211 sample mass (solid curve, left y-axis) and RH (dashed curve, right y-axis) as a function of time.
 212 (b): Change of normalized sample mass as a function of RH when RH decreased linearly from
 213 62% to 54%.

214
 215 A second method has been developed to measure DRH at a given temperature. The particle
 216 sample is first dried at 0% RH until its relative mass change is <0.05% within in 30 min. RH
 217 is then increased to a value which is typically (5-10)% lower than the expected DRH and kept
 218 at this level for 30 min. After that, RH is stepwise increased with an increment of 1% per step,
 219 and at each step RH stays constant for 30 min. The DRH is equal to the RH at which a

220 significant increase in sample mass is first observed. Figure 3 shows changes in RH and
221 normalized sample mass as a function of time in an experiment designed to measure the DRH
222 of $(\text{NH}_4)_2\text{SO}_4$ at 25 °C. As shown in the shadowed region in Figure 3, a sharp increase in
223 normalized sample mass was first observed when RH was increased from 79% to 80%,
224 suggesting that deliquescence of $(\text{NH}_4)_2\text{SO}_4$ occurred between 79% and 80% RH at 25 °C.
225 Further increase in RH from 80% to 81% would cause sharper increase in sample mass,
226 confirming that deliquescence indeed occurred. DRH values measured by the two methods
227 agree with each other, and the second method is preferred because the occurrence of
228 deliquescence can be easily visualized from the experimental data.



229
230 **Figure 3.** Typical experimental data in determination of DRH at a given temperature by
231 stepwise increasing RH. The experiment displayed in this figure was conducted to measure
232 DRH of $(\text{NH}_4)_2\text{SO}_4$ at 25 °C.

233 2.2.2 Quantification of water adsorption and/or mass hygroscopic growth

234 The following experimental procedures are used to determine the amount of water
235 adsorbed by a material (i.e. mass hygroscopic growth factors): 1) a sample pan is delivered into

236 the humidity chamber and temperature in the humidity chamber is set to a given value; 2) after
237 temperature becomes stable, RH in the humidity chamber is set to 0% and the sample is
238 equilibrated with the environment until its mass change is <0.05% within 30 min; 3) RH is
239 increased to a given value and the sample is equilibrated with the environment again until its
240 mass change is smaller than a certain value (typically 0.05% for less hygroscopic materials
241 such as CaCO₃ and fresh soot, and 0.1% for more hygroscopic materials such as (NH₄)₂SO₄
242 and NaCl) within 30 min; 4) RH is further increased to another given value and the sample is
243 equilibrated with the environment. The following assumptions are made to convert the mass of
244 adsorbed water to its surface coverage (Tang et al., 2016): 1) particles are spherical, having a
245 uniform diameter of 1 μm and a density of 2.5 g cm⁻³, and 2) the average surface area that an
246 adsorbed water molecule occupies is 1×10⁻¹⁵ cm². Under these assumptions, a mass change of
247 0.05% (relative to the dry mass) due to adsorption of water is equal to a surface coverage of
248 0.7 monolayers for adsorbed water.

249 All the processes are programmed, with the flexibility to choose the number of RH steps
250 and the corresponding RH values. Experimental data such as RH and sample mass are recorded
251 with a time resolution of 30 s. Relevant experimental results will be presented **and discussed**
252 in Sections 3.3 and 3.4.

253 **2.3 Chemicals**

254 Sodium bromide, provided by TA Instruments as a reference material for RH calibration,
255 was supplied by Alfa Aesar with a stated purity of >99.7%. Ammonium sulfate
256 (purity: >99.0%), sodium chloride (purity: >99.5%), potassium chloride (purity: >99.5%),
257 magnesium nitrate hexahydrate (purity: >99.0%), magnesium chloride hexahydrate
258 (purity: >99.0%), calcium bromide (purity: >99.98%), and calcium sulfate dihydrate
259 (purity: >99%) were purchased from Sigma-Aldrich. All the chemicals were used without
260 further pretreatment.

261 **3 Results and Discussion**

262 **3.1 RH calibration**

263 RH in vapor sorption analyzers and/or thermogravimetric analyzers can be
264 calibrated/verified by determining the DRH of a reference material with a well-defined DRH
265 (ASTM, 2007). In this work, NaBr provided by TA Instruments is used as the reference
266 material (Waguespack and Hesse, 2007). We compare our measured DRHs of NaBr at six
267 different temperatures with those reported by a previous study (Greenspan, 1977). The results
268 are summarized in Table 1, suggesting that the differences between our measured and previous
269 reported DRHs is <1% RH for temperatures ranging from 5 to 30 °C. The agreement is
270 excellent, especially considering that 1) the RH has a stated accuracy of $\pm 1\%$ for our instrument
271 and 2) DRH values reported by Greenspan (1977) typically have errors of $\pm 0.5\%$. Further
272 inspection of results compiled in Table 1 reveals that the difference is larger at lower
273 temperature and becomes smaller at higher temperature.

274

275 **Table 1.** Comparison of DRHs (in %) of NaBr at different temperatures measured in our study
276 with those reported in literature (Greenspan, 1977). **The uncertainties for our measured DRH**
277 **values are estimated to be $\pm 1\%$.**

T (°C)	5	10	15	20	25	30
DRH (literature)	63.5 \pm 0.7	62.2 \pm 0.6	60.7 \pm 0.5	59.1 \pm 0.4	57.6 \pm 0.4	56.0 \pm 0.4
DRH (this work)	62.2	61.2	60.0	58.5	57.6	56.1
difference in DRH	1.3	1.0	0.7	0.6	0.0	-0.1

278

279 DRH values reported by Greenspan (1977), widely accepted as standard values, are
280 recommended by the instrument manufacturer (Waguespack and Hesse, 2007) and also used
281 in this study to calibrate our measure RH by taking into account the difference between our
282 measured DRHs and those reported by Greenspan (1977) for NaBr at different temperatures.

283 All the RHs reported in this work (except measured DRHs of NaBr listed in Table 1) have been
 284 calibrated. In our work we have not verified RH for temperature higher than 30 °C because the
 285 atmospheric relevance is limited. It should be pointed out if necessary, RH calibration can also
 286 be carried out at higher temperature (up to 85 °C) using the same procedure.

287 3.2 DRH measurements

288 Using the experimental method detailed in Section 2.2.1, we have measured DRHs of
 289 CaBr₂, MgCl₂·6H₂O, Mg(NO₃)₂·6H₂O, NaCl, (NH₄)₂SO₄ and KCl at different temperatures
 290 from 5 to 30 °C. All the experimental results are summarized in Table 2. Figure 4a displays our
 291 measured DRHs of these compounds at 25 °C. DRHs range from ~20% to almost 90% for these
 292 six compounds. As evident from Figure 4a, our measured DRHs show excellent agreement
 293 with those reported by a previous study (Greenspan, 1977). Figure 4b shows the comparison
 294 of our measured DRHs with those reported in literature for Mg(NO₃)₂·6H₂O as a function of
 295 temperature (5-30 °C), and excellent agreement is found again. **It also appears that the**
 296 **difference between our measured and previously reported DRH of Mg(NO₃)₂·6H₂O may show**
 297 **a dependence on temperature; however, the difference is not significant compared to**
 298 **uncertainties in DRH measurement.** Careful examination of data compiled in Table 2 suggests
 299 that the absolute difference between our measured and previously reported DRHs is typically
 300 <1%.

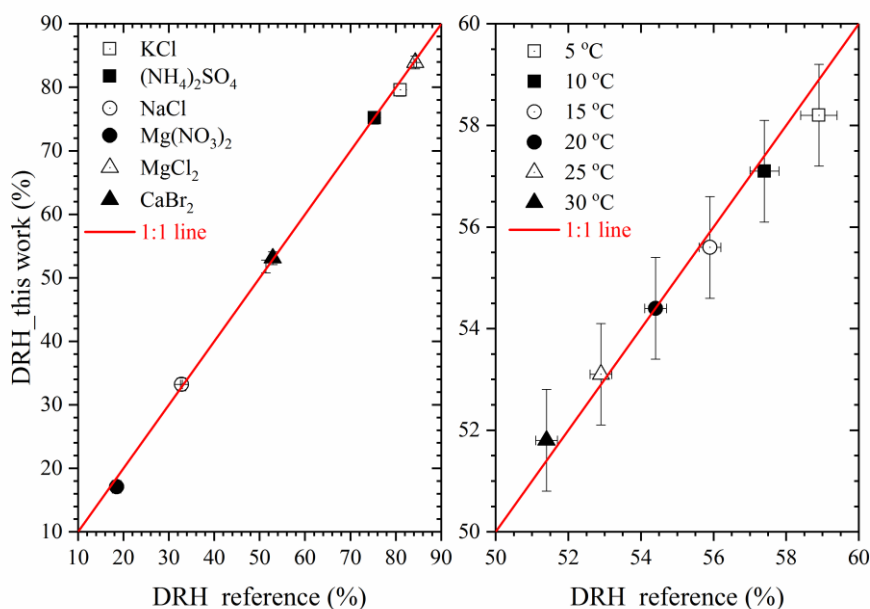
301
 302 **Table 2.** Comparison of DRHs measured by our study with those reported in literature
 303 (Greenspan, 1977) for CaBr₂, MgCl₂·6H₂O, Mg(NO₃)₂·6H₂O, NaCl, (NH₄)₂SO₄ and KCl from
 304 5-30 °C. NA: data are not available. **The uncertainties for our measured DRH values are**
 305 **estimated to be ±1%.**

T (°C)	literature	this work	literature	this work	literature	this work
	CaBr ₂		MgCl ₂ ·6H ₂ O		Mg(NO ₃) ₂ ·6H ₂ O	
5	NA	22.9	33.6±0.3	33.3	58.9±0.5	58.2

10	21.6±0.5	21.6	33.5±0.3	33.9	57.4±0.4	57.1
15	20.2±0.5	20.0	33.3±0.3	33.6	55.9±0.3	55.6
20	18.5±0.5	18.0	33.1±0.2	33.5	54.4±0.3	54.4
25	18.5±0.5	17.1	32.8±0.2	33.2	52.9±0.3	53.1
30	NA	17.7	32.4±0.2	33.6	51.4±0.3	51.8
	NaCl		(NH ₄) ₂ SO ₄		KCl	
5	75.6±0.5	76.0	82.4±0.7	80.8	87.7±0.5	86.7
10	75.7±0.4	75.7	82.1±0.5	80.8	86.8±0.4	86.3
15	75.6±0.3	75.7	81.7±0.4	80.4	85.9±0.4	85.6
20	75.5±0.3	75.6	81.3±0.3	80.3	85.1±0.3	85.0
25	75.3±0.3	75.2	81.0±0.3	79.6	84.3±0.3	83.9
30	75.1±0.3	75.5	80.6±0.3	79.7	83.6±0.3	83.4

306

307 In addition, we repeated the measurements of the DRH of (NH₄)₂SO₄ at 25 °C on several
308 different days, and in total eight measurements have been carried out. The measured DRHs
309 range from 79.5% to 80.1%. Therefore, it can be concluded from our systematical tests that the
310 experimental method developed in our work can reliably measure DRHs from 5 to 30 °C.



311

312 **Figure 4.** Comparison of our measured and previous reported DRHs (Greenspan, 1977). (a)

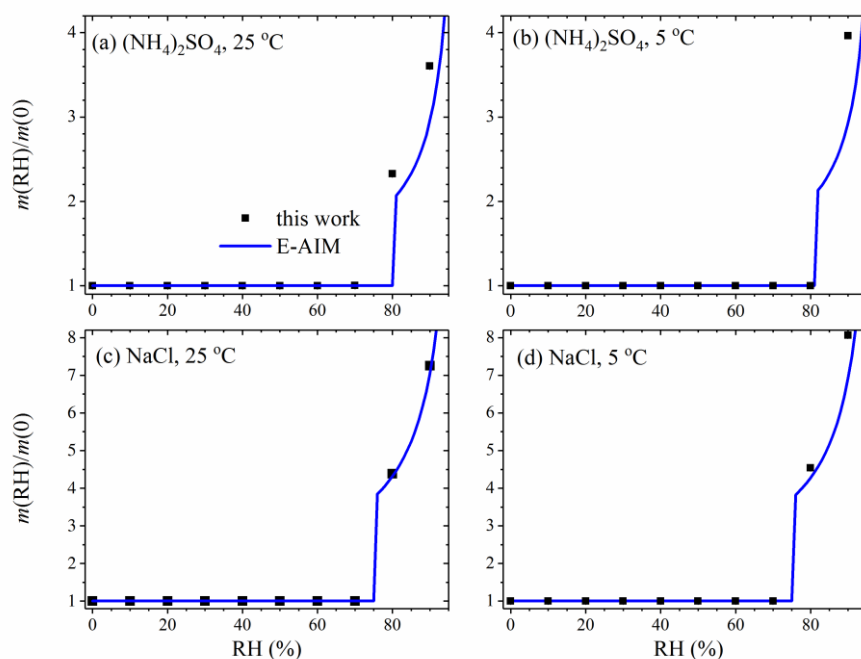
313 DRHs of (NH₄)₂SO₄, NaCl, MgCl₂·6H₂O, Mg(NO₃)₂·6H₂O, CaBr₂ and KCl at 25 °C. **Please**

314 note that error bars are included, but they are too small to be clearly visible. (b) DRHs of
315 $\text{Mg}(\text{NO}_3)_2 \cdot 6\text{H}_2\text{O}$ as a function of temperature from 5-30 °C.

316 **3.3 Mass hygroscopic growth measurements**

317 $(\text{NH}_4)_2\text{SO}_4$ and NaCl are important components found in tropospheric aerosol particles,
318 and their hygroscopicity has been well understood. They have also been widely used as
319 standard materials for validation of hygroscopicity and cloud condensation nucleation activity
320 measurements (Good et al., 2010; Ma et al., 2010b; Tang et al., 2015). In our work we have
321 measured mass hygroscopic growth factors of $(\text{NH}_4)_2\text{SO}_4$ and NaCl as a function of RH at two
322 different temperatures, with the purpose to further assess the performance of our instrument.
323 The mass hygroscopic growth factor is defined as the mass ratio of particles under dry
324 conditions to those at a given RH (Lee et al., 2008; Pope et al., 2010). Figure 5 show the
325 comparison of mass hygroscopic growth factors measured by our work with those predicted by
326 the E-AIM model (Wexler and Clegg, 2002). The agreement between measured and calculated
327 growth factors is excellent for NaCl at both temperatures; for $(\text{NH}_4)_2\text{SO}_4$, the agreement is not
328 as good as NaCl. This may be caused by two reasons. First, after $(\text{NH}_4)_2\text{SO}_4$ is deliquesced,
329 mass hygroscopic growth factors increase sharply with RH, and therefore a small difference in
330 RH would lead a relatively large change in measured mass hygroscopic growth factors; if
331 taking into account the uncertainty in RH ($\pm 1\%$), the difference between our measured and
332 predicted mass hygroscopic growth factors is $<15\%$. Second, inspection of the data in Table 2
333 reveals that the difference between our measured and previously reported DRH is $<1\%$ for all
334 the other compounds except $(\text{NH}_4)_2\text{SO}_4$. This may indicate that the purity of $(\text{NH}_4)_2\text{SO}_4$ could
335 lead to the small but yet detectable difference. In the near future we will purchase $(\text{NH}_4)_2\text{SO}_4$
336 with higher purity and measure its DRH and hygroscopic growth factors. Overall, it can be
337 concluded from the comparison that our measured mass hygroscopic growth factors agree well
338 with theoretical values for $(\text{NH}_4)_2\text{SO}_4$ and NaCl at both 5 and 25 °C. This gives us further

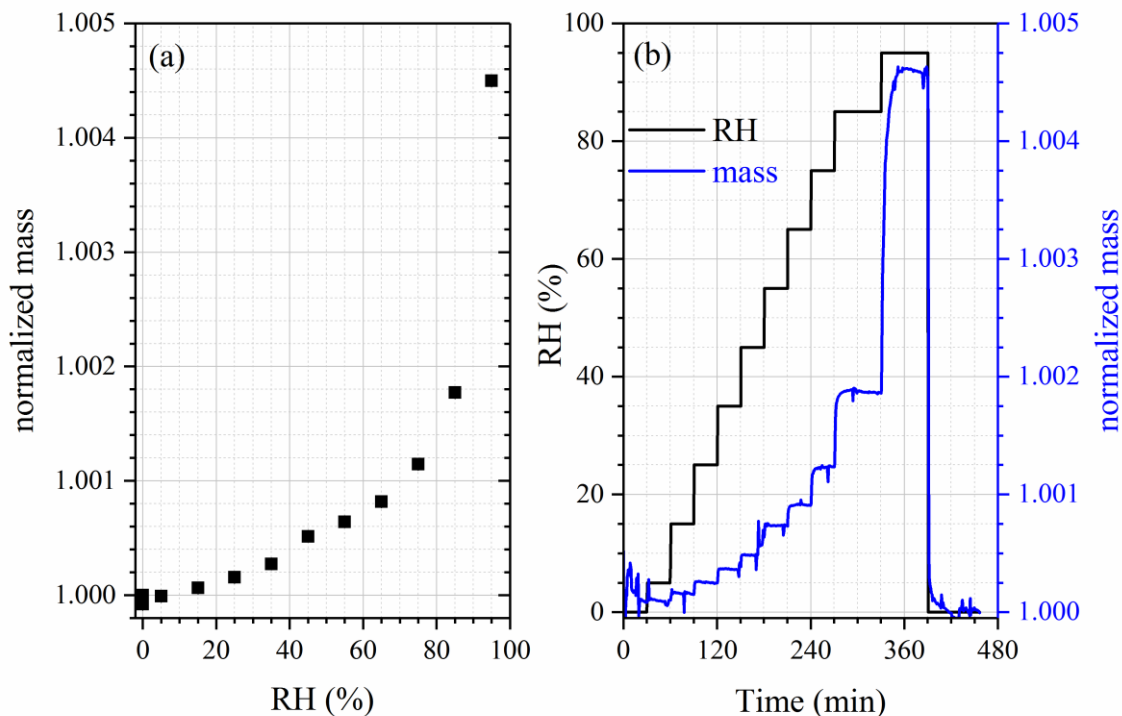
339 confidence that the method developed in this work is reliable for hygroscopicity measurements
340 of atmospheric particles.



341
342 **Figure 5.** Comparison of mass hygroscopic growth factors measured in this work with these
343 predicted by the E-AIM model. (a) $(\text{NH}_4)_2\text{SO}_4$ at 5 °C; (b) $(\text{NH}_4)_2\text{SO}_4$ at 25 °C; (c) NaCl at
344 25 °C; (d) NaCl at 5 °C. **Please note that error bars are included, but they are too small to be**
345 **clearly visible.**

346
347 We have also measured the mass hygroscopic growth factors of $\text{CaSO}_4 \cdot 2\text{H}_2\text{O}$ as a function
348 of RH (up to 95%) at 25 °C. The results are plotted in Figure 6a, and the numerical data are
349 summarized in the appendix (Table A1). As shown in Figure 6, the ability of $\text{CaSO}_4 \cdot 2\text{H}_2\text{O}$ to
350 uptake water is very limited, with the mass ratio of adsorbed water to dry particles determined
351 to be $(0.450 \pm 0.004)\%$ (1σ) at 95% RH. This is qualitatively consistent with two previous
352 studies which suggested that the cloud condensation nucleation activity of calcium sulfate
353 aerosol particles is very low (Sullivan et al., 2009a; Tang et al., 2015). More detailed
354 comparison and discussion are beyond the scope of this paper and will be addressed in a

355 following publication. This also implies that airborne $\text{CaSO}_4 \cdot 2\text{H}_2\text{O}$ particles are not
356 deliquesced for RH up to 95% and therefore may exist as non-spherical particles.



357
358 **Figure 6.** (a) Measured mass hygroscopic growth factors (normalized to the mass at 0% RH)
359 of $\text{CaSO}_4 \cdot 2\text{H}_2\text{O}$ as a function of RH up to 95% RH. Please note that error bars are included,
360 but they are too small to be clearly visible. (b) Time series of RH and normalized mass of
361 $\text{CaSO}_4 \cdot 2\text{H}_2\text{O}$ particles with a dry mass of ~ 9.05 mg during a hygroscopic growth experiment.
362 This experiment was carried out at 25 °C.

363
364 Figure 6b displays change of RH and normalized sample mass with time during the
365 measurement, suggesting that within 6 h our method can measure a relative mass change of
366 $< 0.025\%$. The accuracy of mass measurement is mainly limited by long-term baseline drifts.
367 In another experiment, a CaCO_3 sample (with a dry mass of ~ 10 mg) was used, and its mass
368 was continuously monitored under dry conditions at 25 °C. Under this experimental condition,
369 the baseline drift was determined to be $< 0.05\%$ within 24 h.

370 **4. Conclusion and outlook**

371 The ability to uptake water vapor under subsaturated conditions is one of the most
372 important physicochemical properties of atmospheric particles, largely determining their
373 impacts on atmospheric chemistry and climate. In this work, we have developed a new
374 experimental method to investigate interactions of particles with water vapor under
375 subsaturated conditions at different temperatures from 5 to 30 °C, using a commercial vapor
376 sorption analyzer. Operation temperature can be increased up to 85 °C, though the atmospheric
377 relevance is limited. We have provided a detailed description of instrument configuration as
378 well as experimental procedures to determine DRHs and mass hygroscopic growth factors. For
379 the temperature range we have covered in this work (5-30 °C), our measured DRHs of six
380 different compounds with DRHs ranging from ~20% to ~90%, show excellent agreement with
381 those reported in literature. In addition, mass hygroscopic growth factors measured in our work
382 at different RH values agree well with those predicted by the E-AIM model for (NH₄)₂SO₄ and
383 NaCl at 5 and 25 °C. Therefore, we have demonstrated that experimental methods developed
384 in our work can reliably measure DRHs and mass hygroscopic growth factors from 5 to 30 °C.

385 To test the ability of this instrument to measure hygroscopic growth of compounds with
386 low hygroscopicity, we have determined mass hygroscopic growth factors of CaSO₄·2H₂O at
387 25 °C. It has been found that the ability of CaSO₄·2H₂O to uptake water is very limited. The
388 mass of water adsorbed by CaSO₄·2H₂O at 95% RH is only (0.450±0.004)% of its dry mass. It
389 has also been observed that this instrument can measure a mass change of <0.025% within 6
390 hours and <0.05% within 24 h, and accuracy of mass change determination is mainly limited
391 by baseline drifts. With such an accuracy, this instrument is particularly useful for quantitative
392 determination of water adsorption and/or hygroscopicity of non-spherical particles such as
393 mineral dust and soot. Atmospheric aging processes are known to alter water adsorption,
394 hygroscopicity and cloud condensation nucleation activity of mineral dust and soot particles

395 (Kelly and Wexler, 2005; Laskin et al., 2005; Zhang et al., 2008; Sullivan et al., 2009b; Han et
396 al., 2013; Denjean et al., 2015; Tang et al., 2016). In the future, this instrument will be used to
397 investigate water adsorption and hygroscopicity of mineral dust and soot particles before and
398 after chemical processing. We note that this technique also has a few drawbacks: 1) this
399 technique cannot be used to examine supersaturated droplets or determine efflorescence
400 relative humidities (ERH), due to the contact of particles with the sample pan; 2) substantial
401 amount of particles, typically around or larger than 1 mg, are required by this technique,
402 limiting its application to atmospheric particles even after they are collected (e.g., using a filter
403 or an impactor plate); 3) the experiment is very time-consuming, and a typical experiment can
404 take several hours and even a few days, depending on experimental conditions.

405

406 **Data availability**

407 Experimental data presented in this work are available upon request (Mingjin Tang:
408 mingjintang@gig.ac.cn).

409

410 **Acknowledgement**

411 Financial support provided by Chinese National Science Foundation (grant No.: 91644106 and
412 41675120), Chinese Academy of Sciences international collaborative project (grant No.:
413 132744KYSB20160036) and State Key Laboratory of Organic Geochemistry (grant No.:
414 SKLOGA201603A) is acknowledged. Mingjin Tang would like to thank the CAS Pioneer
415 Hundred Talents program for providing a starting grant and Yongjie Li would like to
416 acknowledge funding support of the Start-up Research Grant from University of Macau
417 (SRG2015-00052-FST). The authors declare no competing financial interest.

418

419 **Appendix**420 **Table A1.** Normalized mass of CaSO₄·2H₂O as a function of RH at 25 °C.

RH (%)	0	5	15	25	35	45
normalized mass	1.00000	0.99999	1.00006	1.00016	1.00027	1.00051
Error	0.00001	0.00002	0.00001	0.00001	0.00004	0.00005
RH (%)	55	65	75	85	95	0
normalized mass	1.00064	1.00082	1.00114	1.00177	1.00450	0.99992
error	0.00002	0.00001	0.00001	0.00001	0.00004	0.00001

421

422 **References**

- 423 Ardon-Dryer, K., Garimella, S., Huang, Y. W., Christopoulos, C., and Cziczo, D. J.:
424 Evaluation of DMA Size Selection of Dry Dispersed Mineral Dust Particles, *Aerosol Sci.*
425 *Technol.*, 49, 828-841, 2015.
- 426 Arenas, K. J. L., Schill, S. R., Malla, A., and Hudson, P. K.: Deliquescence Phase Transition
427 Measurements by Quartz Crystal Microbalance Frequency Shifts, *J. Phys. Chem. A*, 116,
428 7658-7667, 2012.
- 429 ASTM: Standard Test Method for Humidity Calibration (or Conformation) of Humidity
430 Generators for Use with Thermogravimetric Analyzers, American Society for Testing and
431 Materials International, West Conshohocken, PA 19428, USA, doi: 10.1520/E2551-1507,
432 2007.
- 433 Attwood, A. R., and Greenslade, M. E.: Optical Properties and Associated Hygroscopicity of
434 Clay Aerosols, *Aerosol Sci. Technol.*, 45, 1350-1359, 2011.
- 435 Beyer, K. D., Schroeder, J. R., and Kissinger, J. A.: Temperature-Dependent Deliquescence
436 Relative Humidities and Water Activities Using Humidity Controlled Thermogravimetric
437 Analysis with Application to Malonic Acid, *J. Phys. Chem. A*, 118, 2488-2497, 2014.
- 438 Chan, M. N., Kreidenweis, S. M., and Chan, C. K.: Measurements of the hygroscopic and
439 deliquescence properties of organic compounds of different solubilities in water and their
440 relationship with cloud condensation nuclei activities, *Environ. Sci. Technol.*, 42, 3602-3608,
441 2008.
- 442 Clegg, S. L., Brimblecombe, P., and Wexler, A. S.: Thermodynamic Model of the System
443 H⁺-NH₄⁺-Na⁺-SO₄²⁻-NO₃⁻-Cl⁻-H₂O at 298.15 K, *J. Phys. Chem. A*, 102, 2155-2171, 1998.
- 444 Denjean, C., Caquineau, S., Desboeufs, K., Laurent, B., Maille, M., Quiñones Rosado, M.,
445 Vallejo, P., Mayol-Bracero, O. L., and Formenti, P.: Long-range transport across the Atlantic
446 in summertime does not enhance the hygroscopicity of African mineral dust, *Geophys. Res.*
447 *Letts.*, 42, 7835-7843, 2015.
- 448 Estillore, A. D., Hettiyadura, A. P. S., Qin, Z., Leckrone, E., Wombacher, B., Humphry, T.,
449 Stone, E. A., and Grassian, V. H.: Water Uptake and Hygroscopic Growth of Organosulfate
450 Aerosol, *Environ. Sci. Technol.*, 50, 4259-4268, 2016.
- 451 Farmer, D. K., Cappa, C. D., and Kreidenweis, S. M.: Atmospheric Processes and Their
452 Controlling Influence on Cloud Condensation Nuclei Activity, *Chem. Rev.*, 115, 4199-4217,
453 2015.

454 Freedman, M. A., Hasenkopf, C. A., Beaver, M. R., and Tolbert, M. A.: Optical Properties of
455 Internally Mixed Aerosol Particles Composed of Dicarboxylic Acids and Ammonium
456 Sulfate, *J. Phys. Chem. A*, 113, 13584-13592, 2009.

457 Friese, E., and Ebel, A.: Temperature Dependent Thermodynamic Model of the System
458 $H^+-NH_4^+-Na^+-SO_4^{2-}-NO_3^- -Cl^- -H_2O$, *J. Phys. Chem. A.*, 114, 11595-11631, 2010.

459 Frinak, E. K., Mashburn, C. D., Tolbert, M. A., and Toon, O. B.: Infrared characterization of
460 water uptake by low-temperature Na-montmorillonite: Implications for Earth and Mars, *J.*
461 *Geophys. Res.-Atmos.*, 110, D09308, doi: 09310.01029/02004JD005647, 2005.

462 Good, N., Coe, H., and McFiggans, G.: Instrumentational operation and analytical
463 methodology for the reconciliation of aerosol water uptake under sub- and supersaturated
464 conditions, *Atmos. Meas. Tech.*, 3, 1241-1254, 2010.

465 Goodman, A. L., Bernard, E. T., and Grassian, V. H.: Spectroscopic Study of Nitric Acid and
466 Water Adsorption on Oxide Particles: Enhanced Nitric Acid Uptake Kinetics in the Presence
467 of Adsorbed Water, *J. Phys. Chem. A*, 105, 6443-6457, 2001.

468 Greenspan, L.: Humidity fixed points of binary saturated aqueous solutions, *J. Res. Nbs.-A.*
469 *Phys. Chem.*, 81, 89-96, 1977.

470 Griffiths, P. T., Borlace, J. S., Gallimore, P. J., Kalberer, M., Herzog, M., and Pope, F. D.:
471 Hygroscopic growth and cloud activation of pollen: a laboratory and modelling study, *Atmos.*
472 *Sci. Lett.*, 13, 289-295, 2012.

473 Gustafsson, R. J., Orlov, A., Badger, C. L., Griffiths, P. T., Cox, R. A., and Lambert, R. M.:
474 A comprehensive evaluation of water uptake on atmospherically relevant mineral surfaces:
475 DRIFT spectroscopy, thermogravimetric analysis and aerosol growth measurements, *Atmos.*
476 *Chem. Phys.*, 5, 3415-3421, 2005.

477 Han, C., Liu, Y. C., and He, H.: Heterogeneous photochemical aging of soot by NO₂ under
478 simulated sunlight, *Atmos. Environ.*, 64, 270-276, 2013.

479 Herich, H., Tritscher, T., Wiacek, A., Gysel, M., Weingartner, E., Lohmann, U.,
480 Baltensperger, U., and Cziczo, D. J.: Water uptake of clay and desert dust aerosol particles at
481 sub- and supersaturated water vapor conditions, *Phys. Chem. Chem. Phys.*, 11, 7804-7809,
482 2009.

483 Kelly, J. T., and Wexler, A. S.: Thermodynamics of carbonates and hydrates related to
484 heterogeneous reactions involving mineral aerosol, *J. Geophys. Res.-Atmos*, 110, D11201,
485 doi: 11210.11029/12004jd005583, 2005.

486 Koehler, K. A., Kreidenweis, S. M., DeMott, P. J., Petters, M. D., Prenni, A. J., and Carrico,
487 C. M.: Hygroscopicity and cloud droplet activation of mineral dust aerosol, *Geophys. Res.*
488 *Lett.*, 36, L08805, doi: 08810.01029/02009gl037348, 2009.

489 Krieger, U. K., Marcolli, C., and Reid, J. P.: Exploring the complexity of aerosol particle
490 properties and processes using single particle techniques, *Chem. Soc. Rev.*, 41, 6631-6662,
491 2012.

492 Laskin, A., Iedema, M. J., Ichkovich, A., Graber, E. R., Taraniuk, I., and Rudich, Y.: Direct
493 Observation of Completely Processed Calcium Carbonate Dust Particles, *Faraday Discuss.*,
494 130, 453-468, 2005.

495 Lee, A. K. Y., Ling, T. Y., and Chan, C. K.: Understanding hygroscopic growth and phase
496 transformation of aerosols using single particle Raman spectroscopy in an electrodynamic
497 balance, *Faraday Discuss.*, 137, 245-263, 2008.

498 Lei, T., Zuend, A., Wang, W. G., Zhang, Y. H., and Ge, M. F.: Hygroscopicity of organic
499 compounds from biomass burning and their influence on the water uptake of mixed organic
500 ammonium sulfate aerosols, *Atmos. Chem. Phys.*, 14, 11165-11183, 2014.

501 Liu, P. F., Li, Y. J., Wang, Y., Gilles, M. K., Zaveri, R. A., Bertram, A. K., and Martin, S. T.:
502 Lability of secondary organic particulate matter, *Proc. Natl. Acad. Sci. U. S. A.*, 113, 12643-
503 12648, 2016.

504 Ma, Q. X., He, H., and Liu, Y. C.: In Situ DRIFTS Study of Hygroscopic Behavior of
505 Mineral Aerosol, *J. Environ. Sci.*, 22, 555-560, 2010a.

506 Ma, Q. X., Liu, Y. C., and He, H.: The Utilization of Physisorption Analyzer for Studying the
507 Hygroscopic Properties of Atmospheric Relevant Particles, *J. Phys. Chem. A*, 114, 4232-
508 4237, 2010b.

509 Ma, Q. X., Liu, Y. C., Liu, C., and He, H.: Heterogeneous Reaction of Acetic Acid on MgO,
510 α -Al₂O₃, and CaCO₃ and the Effect on the Hygroscopic Behavior of These Particles, *Phys.*
511 *Chem. Chem. Phys.*, 14, 8403-8409, 2012.

512 Martin, S. T.: Phase transitions of aqueous atmospheric particles, *Chem. Rev.*, 100, 3403-
513 3453, 2000.

514 McFiggans, G., Artaxo, P., Baltensperger, U., Coe, H., Facchini, M. C., Feingold, G., Fuzzi,
515 S., Gysel, M., Laaksonen, A., Lohmann, U., Mentel, T. F., Murphy, D. M., O'Dowd, C. D.,
516 Snider, J. R., and Weingartner, E.: The effect of physical and chemical aerosol properties on
517 warm cloud droplet activation, *Atmos. Chem. Phys.*, 6, 2593-2649, 2006.

518 Pöschl, U.: Atmospheric Aerosols: Composition, Transformation, Climate and Health
519 Effects, *Angew. Chem.-Int. Edit.*, 44, 7520-7540, 2005.

520 Petters, M. D., and Kreidenweis, S. M.: A single parameter representation of hygroscopic
521 growth and cloud condensation nucleus activity, *Atmos. Chem. Phys.*, 7, 1961-1971, 2007.

522 Pope, F. D.: Pollen grains are efficient cloud condensation nuclei, *Environ. Res. Lett.*, 5,
523 044015, 2010.

524 Pope, F. D., Dennis-Smith, B. J., Griffiths, P. T., Clegg, S. L., and Cox, R. A.: Studies of
525 Single Aerosol Particles Containing Malonic Acid, Glutaric Acid, and Their Mixtures with
526 Sodium Chloride. I. Hygroscopic Growth, *J. Phys. Chem. A*, 114, 5335-5341, 2010.

527 Pruppacher, H. R., and Klett, J. D.: *Microphysics of Clouds and Precipitation*, Kluwer
528 Academic Publishers, Dordrecht, Netherlands 1994.

529 Robinson, C. B., Schill, G. P., Zarzana, K. J., and Tolbert, M. A.: Impact of Organic Coating
530 on Optical Growth of Ammonium Sulfate Particles, *Environ. Sci. Technol.*, 47, 13339-13346,
531 2013.

532 Rubasinghege, G., and Grassian, V. H.: Role(s) of Adsorbed Water in the Surface Chemistry
533 of Environmental Interfaces, *Chem. Commun.*, 49, 3071-3094, 2013.

534 Schroeder, J. R., and Beyer, K. D.: Deliquescence Relative Humidities of Organic and
535 Inorganic Salts Important in the Atmosphere, *J. Phys. Chem. A*, 120, 9948-9957, 2016.

536 Schuttlefield, J., Al-Hosney, H., Zachariah, A., and Grassian, V. H.: Attenuated Total
537 Reflection Fourier Transform Infrared Spectroscopy to Investigate Water Uptake and Phase
538 Transitions in Atmospherically Relevant Particles, *Appl. Spectrosc.*, 61, 283-292, 2007a.

539 Schuttlefield, J. D., Cox, D., and Grassian, V. H.: An investigation of water uptake on clays
540 minerals using ATR-FTIR spectroscopy coupled with quartz crystal microbalance
541 measurements, *J. Geophys. Res.-Atmos.*, 112, D21303, doi: 21310.21029/22007JD008973,
542 2007b.

543 Seinfeld, J. H., and Pandis, S. N.: *Atmospheric Chemistry and Physics: From Air Pollution to*
544 *Climate Change*, Wiley Interscience, New York, 2006.

545 Sullivan, R. C., Moore, M. J. K., Petters, M. D., Kreidenweis, S. M., Roberts, G. C., and
546 Prather, K. A.: Effect of Chemical Mixing State on the Hygroscopicity and Cloud Nucleation
547 Properties of Calcium Mineral Dust Particles, *Atmos. Chem. Phys.*, 9, 3303-3316, 2009a.

548 Sullivan, R. C., Moore, M. J. K., Petters, M. D., Kreidenweis, S. M., Roberts, G. C., and
549 Prather, K. A.: Timescale for Hygroscopic Conversion of Calcite Mineral Particles through
550 Heterogeneous Reaction with Nitric Acid, *Phys. Chem. Chem. Phys.*, 11, 7826-7837, 2009b.

551 Swietlicki, E., Hansson, H. C., Hameri, K., Svenningsson, B., Massling, A., McFiggans, G.,
552 McMurry, P. H., Petaja, T., Tunved, P., Gysel, M., Topping, D., Weingartner, E.,
553 Baltensperger, U., Rissler, J., Wiedensohler, A., and Kulmala, M.: Hygroscopic properties of

554 submicrometer atmospheric aerosol particles measured with H-TDMA instruments in various
555 environments - a review, *Tellus Ser. B-Chem. Phys. Meteorol.*, 60, 432-469, 2008.

556 Tang, M. J., Whitehead, J., Davidson, N. M., Pope, F. D., Alfarra, M. R., McFiggans, G., and
557 Kalberer, M.: Cloud Condensation Nucleation Activities of Calcium Carbonate and its
558 Atmospheric Ageing Products, *Phys. Chem. Chem. Phys.*, 17, 32194-32203, 2015.

559 Tang, M. J., Czikzo, D. J., and Grassian, V. H.: Interactions of Water with Mineral Dust
560 Aerosol: Water Adsorption, Hygroscopicity, Cloud Condensation and Ice Nucleation, *Chem.*
561 *Rev.*, 116, 4205–4259, 2016.

562 Vali, G., DeMott, P. J., Möhler, O., and Whale, T. F.: Technical Note: A proposal for ice
563 nucleation terminology, *Atmos. Chem. Phys.*, 15, 10263-10270, 2015.

564 Veghte, D. P., and Freedman, M. A.: The Necessity of Microscopy to Characterize the
565 Optical Properties of Size-Selected, Nonspherical Aerosol Particles, *Anal. Chem.*, 84, 9101-
566 9108, 2012.

567 Vlasenko, A., Sjogren, S., Weingartner, E., Gaggeler, H. W., and Ammann, M.: Generation
568 of submicron Arizona test dust aerosol: Chemical and hygroscopic properties, *Aerosol Sci.*
569 *Technol.*, 39, 452-460, 2005.

570 Waguespack, L., and Hesse, N.: TN66: Humidity Calibration of Dynamic Vapor Sorption
571 (DVS) Instruments, TA Instruments, New Castle, DE 19720, USA, 2007.

572 Wexler, A. S., and Clegg, S. L.: Atmospheric aerosol models for systems including the ions
573 H^+ , NH_4^+ , Na^+ , SO_4^{2-} , NO_3^- , Cl^- , Br^- , and H_2O , *J. Geophys. Res.-Atmos*, 107, 4207, doi:
574 4210.1029/2001JD000451, 2002.

575 Wu, Z. J., Nowak, A., Poulain, L., Herrmann, H., and Wiedensohler, A.: Hygroscopic
576 behavior of atmospherically relevant water-soluble carboxylic salts and their influence on the
577 water uptake of ammonium sulfate, *Atmos. Chem. Phys.*, 11, 12617-12626, 2011.

578 Yeşilbaş, M., and Boily, J.-F.: Particle Size Controls on Water Adsorption and Condensation
579 Regimes at Mineral Surfaces, *Scientific Reports*, 6, 32136, doi: 32110.31038/srep32136,
580 2016.

581 Zhang, R. Y., Khalizov, A. F., Pagels, J., Zhang, D., Xue, H. X., and McMurry, P. H.:
582 Variability in morphology, hygroscopicity, and optical properties of soot aerosols during
583 atmospheric processing, *Proc. Natl. Acad. Sci. U. S. A.*, 105, 10291-10296, 2008.

584